

Observations at Venus Encounter by the Plasma Science Experiment on Mariner 10

Abstract. Preliminary results from the rearward-looking electrostatic analyzer of the plasma science experiment during the Mariner 10 encounter with Venus are described. They show that the solar-wind interaction with the planet probably involves a bow shock rather than an extended exosphere, but that this is not a thin boundary at the point where it was crossed by Mariner 10. An observed reduction in the flux of electrons with energies greater than 100 electron volts is interpreted as evidence for some direct interaction with the exosphere. Unusual intermittent features observed downstream of the planet indicate the presence of a comet-like tail hundreds of scale lengths in length.

The plasma science experiment is a cooperative effort by groups from the Massachusetts Institute of Technology, the Los Alamos Scientific Laboratory, the Goddard Space Flight Center, and the University of California at Los Angeles. The instrument consists of two independent hemispherical electrostatic analyzers mounted back-to-back on a scan platform. The platform moves through an arc of 120 deg centered on a direction in the ecliptic plane, 10 deg east of the spacecraft-sun line. The platform axis is pointed toward Canopus, approximately perpendicular to the plane of the ecliptic. We report here results from the rearward-looking analyzer, which accepts electrons in the energy (E) range from 13 to 715 ev in 15 logarithmically spaced windows of width $\Delta E/E = 6.6$ percent. The field of view is fan-shaped: ± 3.5 deg in the scan plane and ± 13.5 deg perpendicular to that plane. The instrument obtains an electron spectrum every 6 seconds, measuring at each differential energy step for 0.4 second. The sunward-facing analyzer was designed to accept electrons and positive ions, but, unfortunately, no data have yet been obtained from it because of some presently unexplained electrical or mechanical failure.

We present preliminary measurements of electron number density and temperature; flow speed and temperature anisotropy measurements will eventually be available from this instrument for times when it was in the interplanetary medium and perhaps in the vicinity of the planets. These are the first measurements of plasma electrons near Venus, and we show that they can be interpreted in such a way as to add considerably to our knowledge of the planet.

Figures 1 and 2 show the Mariner 10 trajectory and the plasma electron observations during the period from 1530 U.T. to 1800 U.T., spacecraft time (that is, the universal time at

which the corresponding datum was taken by the spacecraft). Periapasis was at 1701:50 U.T. when the spacecraft was 11,858 km from the center of the planet. The trajectory of the 1967 encounter of Mariner 5 with Venus is also shown for comparison. The observed fluxes of electrons in the energy ranges from 12.9 to 13.8 ev and from 501 to 535 ev are shown, as well as the values of density and temperature derived from these and the other differential channels by the methods outlined in the caption for Fig. 2 and described in (1) (the bulk speed effects have not been removed; consequently, peak values of the densities are most representative of the plasma environment and the best temperature estimates occur at these times also).

These two channels were chosen to provide representative observations at low and high energies, respectively. The events in Fig. 1 are plotted as a function of time (in minutes) with zero at the time of periapsis, whereas those in Fig. 2 are in spacecraft time. Six features of interest are identified by letters in the data fields, corresponding to the same lettered locations on the trajectory.

Each of the trajectories is plotted in the rotating plane containing the sun, the center of the planet, and the spacecraft, so that the plot gives the distance of the spacecraft from the sun-Venus line as a function of its motion along that line. This coordinate system is the appropriate one if the solar wind interaction is axially symmetric about the sun-Venus line. However, we note that the solar wind direction can deviate several degrees from this line, so that the interaction features may not be axially symmetric by this amount. The aberrated flow direction of the free-streaming solar wind was 4 deg from the west after encounter; the solar wind direction at the time of the encounter of Mariner 5 was inferred from upstream observations to be 4 ± 1 deg from the west. Figure 1 shows two calculated bow shock and ionopause locations. The

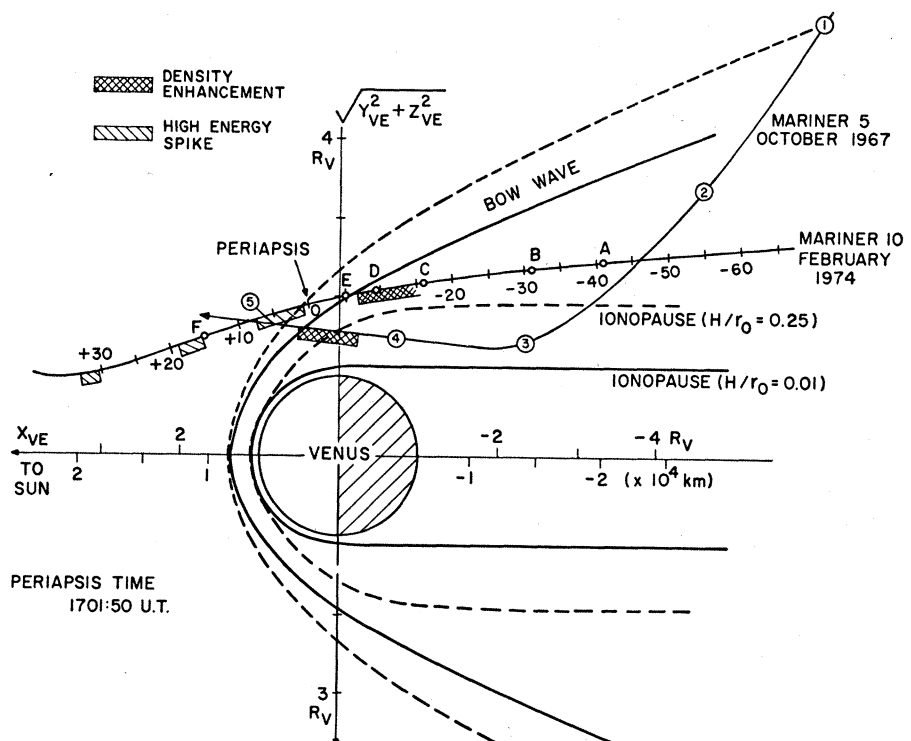


Fig. 1. The Mariner 10 and Mariner 5 trajectories in a plane containing the Venus-sun line. The planet and two predictions of fluid theory for the case of flow along the Venus-sun line are also shown. The letters refer to events along the track of Mariner 10, and the circled numbers refer to events along the track of Mariner 5.

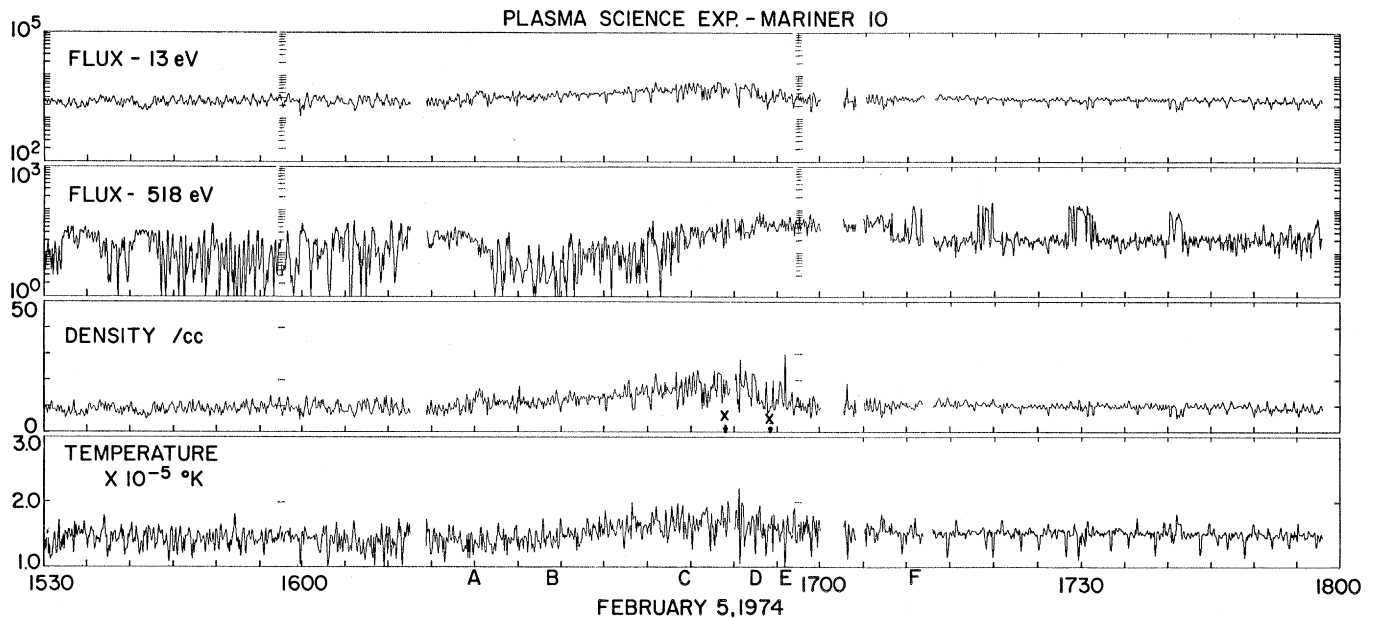


Fig. 2. The data fields show the fluxes observed at 13 and 518 eV, respectively, and also plots of "density" and "temperature." The density is defined as $(4\pi/\Delta\Omega) \int f dv$ and the temperature as $2\pi m_e/\Delta\Omega \int f v^2 dv$ where the integrations have been carried out numerically for the spectra between 0 and 40 eV observed by the detector, which has a solid angle of acceptance of $\Delta\Omega$. The necessary extrapolation between 13 eV and zero is made by assuming a Maxwellian form for the spectrum.

dashed lines are those which were proposed as a representative model of the Mariner 5 data, whereas the solid lines correspond to one model from a parameter study (2).

As the planet is approached, the density generally increases, reaching a maximum about 10 minutes before periapsis, and then drops rapidly to half its maximum value. Throughout the encounter period the density never decreases substantially below the upstream solar wind value of approximately ten electrons per cubic centimeter. Superimposed upon this broad density feature are many large-amplitude, short-period variations which suggests the presence of turbulent flow. The electron distribution functions always decrease monotonically toward higher energies (Fig. 3); low-energy flux channels usually control the densities. Some aliasing may have occurred in the period (from x to x) indicated in Fig. 2. After the density decrease, there are several discontinuous density increases, up to the last density "spike," labeled event E in Fig. 2.

New features are seen in the data from the high-energy channel. At the beginning of the gradual rise in density, the flux at high energy begins to decrease rather rapidly (event A). After 9 minutes, the high-energy flux reaches a minimum (event B) and then rises to the predecrease value after 15 minutes (event C). Point C

occurs 8 minutes before the density decrease (event D). At its minimum, the flux in the high-energy channel is about one-fifth as much as its value in the upstream solar wind, and this feature is general in channels above ~ 100 eV. The flux in this energetic electron "bite out" interval is highly modulated at the scan frequency, implying a large anisotropy; that is, the flux is very directional. Several smaller decreases, of short duration, occurred in high-energy channels before event A. Figure 4 shows a comparison between the electron distribution functions observed before and during the decrease in high-energy flux.

Another noteworthy feature is that for electron energies above about 100 eV, the flux increases across the discontinuity D, whereas for lower energies it decreases markedly. The energetic electron flux drops to the ambient solar wind value at event F. There are four brief occurrences of the high, upstream, energetic electron fluxes within 35 minutes after event E, each about 2 minutes in duration. Their locations are shown on the Mariner 10 trajectory in Fig. 1.

The temperature parameter shown in the last data field is based on electrons with energies less than 40 eV to avoid biasing by the nonthermal, energetic electron fluxes. The variation in temperature is smaller than the variation in any other parameter. There is a small increase coinciding in shape

with the broad density feature and exhibiting a total range of a factor of 1.3.

We now compare these results with those of Mariner 5; five features were discussed by the Mariner 5 experimenters (3), denoted by circled numbers in Fig. 1. Feature 1 was identified with the crossing of a bow wave. The trajectory of Mariner 10 is such that it would have crossed a bow wave far downstream, and no clear crossing analogous to that at feature 1 was observed. Feature 2 marked a decrease in $|\bar{B}|$, a change in the character of the magnetic fluctuations, and a drop in density and flow speed. The flow speed dropped to its lowest value at feature 3, abruptly recovering at feature 4. From detailed examinations of the plasma and magnetic field records, the spacecraft is thought to have passed through a shock transition between features 4 and 5.

The plasma and magnetometer data observed at Mariner 5 and Mariner 10 encounters raise the obvious question: Do the density, temperature, and magnetic field enhancements along with the accompanying large-amplitude and high-frequency fluctuations occurring between events C and E during the Mariner 10 encounter and between features 4 and 5 during the Mariner 5 encounter represent the signature of a standing bow shock? The Mariner 5 investigators interpreted such fea-

tures as representative of a bow shock, and several subsequent models (4) showed that it is plausible to expect a shock when the solar wind interacts with a planetary ionosphere. An alternative interpretation is that no shock was present and that the above-mentioned features correspond to the effects of planetary ions picked up by the wind far upstream of the planet (5). We shall consider both possibilities in what follows.

By representing the interface between the solar wind and the ionosphere (ionopause) as a tangential discontinuity, a detailed fluid dynamic model has been constructed to explain the Mariner 5 data for the solar wind interaction with Venus (2). The ionopause surface was determined by requiring a balance between the solar wind ram pressure and the topside ionospheric pressure. In this model the ionosphere was characterized by H/r_0 , the ratio of the ionospheric scale height $H = k(T_e + T_i)/m_i g$ to the planetocentric distance r_0 of the nose of the ionopause, where k is Boltzmann's constant; T_e and T_i are, respectively, the electron and ion temperatures of the topside ionosphere; m_i is the ion mass; and g is the gravitational acceleration. A best representation of the Mariner 5 bow shock position was obtained (2) for $H/r_0 = 0.25$, and we note that this model represents a rather poor prediction of the shock positions suggested by Mariner 10, which lie essentially midway between the theoretical ionopause and bow shock. The following considerations tend to alleviate this problem: (i) the theoretical shape of the ionopause ($H/r_0 = 0.25$) is inappropriate for Mariner 10 (and possibly Mariner 5); (ii) the location of the bow shock depends upon the immediate history of the flow direction of the solar wind; and (iii) the addition of solar wind material to the Venus atmosphere will alter the shock position.

Even without the stimulus of the Mariner 10 observations, one can argue that the shape of the ionopause should be modified to account for the expected ionospheric temperature decrease from the subsolar point to the terminator; that is, H/r_0 is expected to decrease with increasing solar zenith angle. This modification alone makes the obstacle to the solar wind smaller (lower average radius of curvature on the day-side), thereby bringing the shock closer to the planetary surface in the terminator plane. In addition, the ram pressure of the solar wind during the

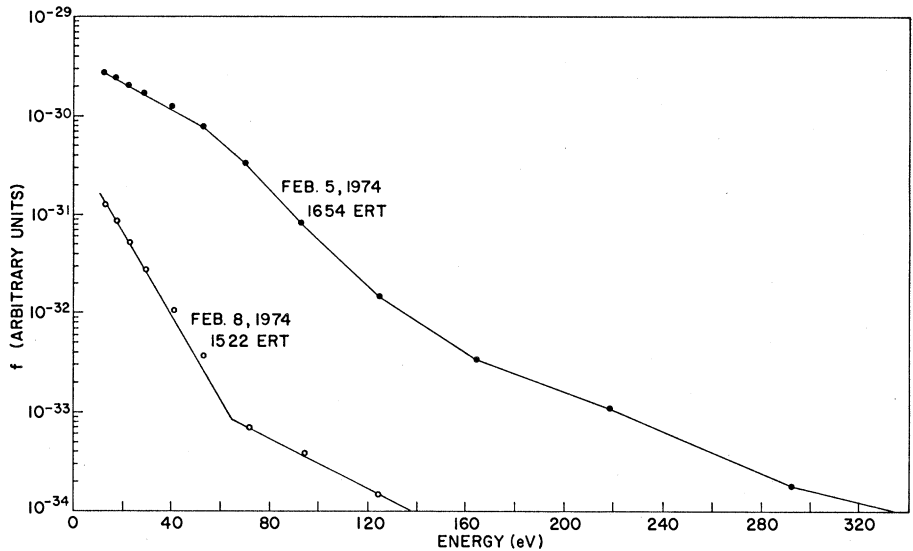


Fig. 3. A comparison of the measured energy distribution function in the maximum density region (near point D of Fig. 2) with a typical upstream solar wind spectrum taken on 8 February 1974. A fit to a straight line indicates a Maxwellian distribution function. The solar wind spectrum is adequately represented by a sum of two Maxwellians, whereas the maximum density spectrum is not; ERT, Earth real time.

Mariner 10 encounter was most probably about a factor of 1.5 greater than that during the Mariner 5 encounter; this suggests that the light ions of the topside ionosphere (inferred from Mariner 5 data) may have been compressed and perhaps squeezed laterally into the tail, thereby reducing the altitude of the dayside ionopause relative to that for Mariner 5, decreasing its radius of curvature. The solar wind ram pressure was approximately twice as high before the Mariner 10 encounter which may have "pushed" the ionopause into the main part of the ionosphere consisting of O_2^+ and CO_2^+ . Thus, the combined

effects of accounting for a cooler ionospheric plasma at the terminator and a higher solar wind ram pressure during the Mariner 10 encounter should result in a smaller obstacle in the wind than previously supposed. With this in mind, we have attempted to fit the presumed Mariner 10 shock crossing by selecting a fluid interaction model (2) with $H/r_0 = 0.01$ as indicated in Fig. 1 (the low value for H/r_0 we have chosen is intended to account for the cool terminator region although the shape of the ionopause over a large portion of the dayside is rather insensitive to the value chosen; on this basis we have chosen a constant value

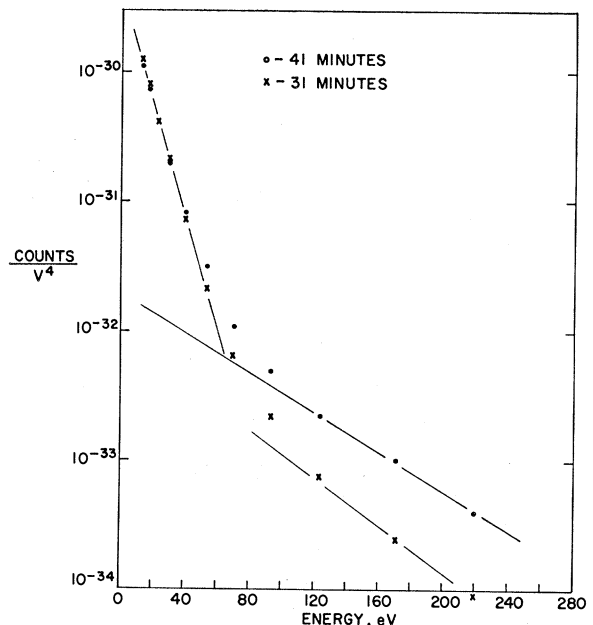


Fig. 4. Two electron spectra showing distribution functions before, — 41 minutes, and during, — 31 minutes, the decrease in high-energy flux, points A through C in Fig. 1.

for H/r_0). We note that this results in a considerably improved fit to the density maximum positions measured by Mariner 10. A lower value of H/r_0 is suggestive of an effective ion mass $m_i > m_1$ (He^+) near the ionopause (perhaps O^+ and O_2^+ , which is consistent with several models of the top-side ionosphere) (6).

A shock wave can have high-amplitude standing waves on the downstream side and may be in motion; thus, the apparent lack of sharpness of the discontinuity at event D may be related to downstream waves or to the motion of the shock. Furthermore, when the interplanetary magnetic field is parallel to its normal, Earth's bow shock has been observed to be pulsating (7), and this could also occur in the case of the Venus bow wave. The effective shape of the obstacle should be approximately spherical (even for large deviations in the flow direction of the free-streaming solar wind), and thus the position and movement of the shock would be sensitive to the direction and directional changes in the flow of the free-streaming solar wind. This may be an additional cause of the density peaks near event D. The fluid interaction models with $H/r_0 < 0.25$ may be applicable for the Mariner 5 encounter, since the apparent solar wind flow direction was from the west of the sun during the shock crossing at feature 1 and a value of $H/r_0 < 0.25$ would be needed for the theoretical position of the shock to pass through the crossing at feature 1 and the density maximum preceding feature 5.

In addition to the dependence on the direction of solar-wind flow, the shock position also depends on solar wind penetration into the dayside ionosphere. If a fraction of the solar wind is absorbed by the ionosphere, then the standoff distance will decrease since less plasma is diverted around the planet. We note that such penetration of solar wind is also desirable from the standpoint of several models of the dayside ionosphere (6) which require an additional ionization source to explain the peak ion concentration of the " F_1 layer."

Altogether, it appears that the salient features of both the Mariner 10 and Mariner 5 plasma data taken during their respective encounters can be understood in terms of a fluid interaction of the solar wind with the ionosphere of Venus and that corresponding models

are consistent with the presence of a standing bow wave which can pass through the high-density regions observed by both spacecraft. Thus, it appears that there is no need for a hot ($> 1500^\circ\text{K}$) extended neutral exosphere as has been proposed to slow the solar wind down far upstream of the planet (by means of mass loading due to planetary ions born in the wind) in order to avoid the formation of a bow shock. This conclusion is also consistent with the low exospheric temperatures inferred from both Mariner 10 ($\approx 400^\circ\text{K}$) (8) and Mariner 5 ($600^\circ \pm 50^\circ\text{K}$) (9) as well as calculated upper bounds on the extent of the neutral atmosphere and ion-exosphere in the solar wind (10). Additional support for a bow shock is provided by the observation of the high-energy electron enhancements, upstream of the planet, similar to those observed near Earth's bow shock.

We suggest that the flux decrease observed at energies above 100 eV, when the spacecraft was between events A and C on its trajectory, was caused by depletion of the electron population on magnetic flux tubes which passed close to the ionopause. Since the cross section for electron impact ionization of helium has a peak near 100 eV and remains high above that energy, penetration into the neutral helium exosphere is a natural way for electrons at these energies to be selectively removed or to have their pitch angle distribution disturbed. This is consistent with the observed flux modulation. Considering the probable dimensions of the interaction region near the ionopause, a helium density of 10^6 to 10^7 per cubic centimeter is sufficient for the high-energy electron depletion observed, and such densities have been predicted at the altitude of the ionopause (6).

The interaction between the solar wind and the Venusian atmosphere appears to resemble in some ways that thought to occur with a comet. This is supported by the possible penetration of solar wind into the atmosphere of Venus and the depletion of high-energy electrons as they pass through the exosphere near the ionopause. In addition, unusual intermittent features unlike those observed in the terrestrial magnetosheath or in the free-streaming solar wind were observed thousands of scale lengths downstream of Venus during the approach of Mariner 10.

The following conclusions may be

drawn from the data presented here: (i) the interaction of the solar wind with Venus most probably results in a bow shock; the best fit by hydrodynamic models at the time of Mariner 10 is characterized by $H/r_0 = 0.01$; (ii) an extended exosphere which slows down the solar wind without a bow shock appears very unlikely; (iii) a direct interaction between the solar wind and the Venusian atmosphere is indicated by the behavior of electrons of energy between 100 and 500 eV; and (iv) Venus probably has a "tail" hundreds of scale lengths long, suggestive of that of a comet.

H. S. BRIDGE, A. J. LAZARUS
Center for Space Research and
Department of Physics, Massachusetts
Institute of Technology, Cambridge

J. D. SCUDDER, K. W. OGLIVIE
Laboratory for Extraterrestrial
Physics, Goddard Space Flight
Center, Greenbelt, Maryland 20771

R. E. HARTLE
Laboratory for Planetary Atmospheres,
Goddard Space Flight Center

J. R. ASBRIDGE, S. J. BAME
W. C. FELDMAN
University of California Los Alamos
Scientific Laboratory,
Los Alamos, New Mexico

G. L. SISCOE
Department of Meteorology,
University of California, Los Angeles

References and Notes

1. J. D. Scudder, D. L. Lind, K. W. Ogilvie, *J. Geophys. Res.* **78**, 6535 (1973).
2. J. R. Spreiter, A. L. Summers, A. W. Rizzi, *Planet. Space Sci.* **18**, 1281 (1970).
3. H. S. Bridge, A. J. Lazarus, C. W. Snyder, E. J. Smith, L. Davis, Jr., P. J. Coleman, Jr., D. E. Jones, *Science* **158**, 1669 (1967).
4. A. J. Dessler, in *Atmospheres at Mars and Venus*, J. C. Brandt and M. B. McElroy, Eds. (Gordon and Breach, New York, 1968), pp. 241-250; F. S. Johnson and J. E. Midgley, in *Space Research 9*, K. S. Champion et al., Eds. (North-Holland, Amsterdam, 1969), p. 760.
5. M. K. Wallis, *Cosmic Electrodyn.* **3**, 45 (1972).
6. S. J. Bauer, *Physics of Planetary Ionospheres* (Springer-Verlag, New York, 1973).
7. E. W. Greenstadt, *J. Geophys. Res.* **77**, 1729 (1972); D. H. Fairfield, *ibid.* **74**, 3541 (1969); *ibid.*, in press.
8. L. Broadfoot et al., *Science* **183**, 1315 (1974).
9. C. A. Barth, J. B. Pearce, K. K. Kelly, L. Wallace, W. G. Fastie, *ibid.* **158**, 1675 (1967).
10. R. E. Hartle, S. J. Bauer, C. S. Wu, *Int. Ass. Geophys. Aeron. Bull.* **34**, 569 (1973).
11. We cannot acknowledge by name everyone who worked so well to make this experiment possible, but we would like to mention the following: R. Butler, E. Hu, and A. Mavretic at MIT; M. Acuna, H. Doong, J. Sites, H. Burdick, R. Hoffman, and T. Carleton at Goddard Space Flight Center; P. Glore, E. Engelke, and E. Tech at Los Alamos Scientific Laboratory; and C. Yeates, J. Dunne, D. Swenson, and J. Tupman at the Jet Propulsion Laboratory. Special thanks are due to K. Nakagawa for his efforts as cognizant engineer. The plasma team would like to acknowledge several useful discussions with the magnetometer team on Mariner 10.

4 March 1974